PHYSICAL REVIEW A VOLUME 5, NUMBER 3 MARCH 1972

Ionization of Multielectron Atoms by Fast Charged Particles

K. Omidvar, H. L. Kyle, and E. C. Sullivan
Theoretical Studies Branch, *NASA–Goddard Space Flight Center*, *Greenbelt*, *Maryland* 20771
(Received 5 May 1971; revised manuscript received 27 September 1971)

Using plane waves to describe the incident and scattered particles, and screened hydrogenic and Coulomb functions to describe the atomic electrons before and after ejections, we have calculated the differential and total ionization cross sections of 11 atoms and one ion by electron impact, and ionization of helium by proton impact. The effective charges of the screened hydrogenic functions are fixed by the Hartree-Fock calculations. Calculations have been carried out for the atomic s, p, and d electrons. For low atomic numbers we find reasonable agreement with the experimental data. For intermediate atomic numbers we expect our results to overestimate the actual cross sections, since our choice of a unit charge for the Coulomb function of the ejected electrons will overestimate the atomic dipole potential strength, and in turn the high-energy cross sections. Our results agree closely with the calculational results of Peach, based on a model similar to ours except that the atomic electrons before ejections are described by the Hartree-Fock wave functions. For intermediate atomic numbers and inert gases, the calculated results of McGuire seems to agree better with the experimental data compared to other calculations. The advantage of the method presented here is that the ionization amplitude is given in analytic form. This may allow further analysis on this amplitude, and facilitates extension of the numerical integration for the cross section to high impact energies. We have also given some cross sections for the production of doubly charged ions due to the single ionization.

I. INTRODUCTION

Based on a model which will be described below, we have calculated ionization cross sections of 11 atoms and one ion by electron impact, and ionization of helium by proton impact. Some of the results have been reported previously.[1] Calculation is in the Born approximation. It is assumed that in the ionization process the incident particle interacts only with a single electron in the target atom or ion. The active electron in the target atom or ion is described by screened hydrogenic functions before ejection, and by a Coulomb function with the charge unity after ejection. Calculations are carried out for s, p, and d atomic electrons. Calculation on atomic d electrons apparently has not been carried out before.

Similar calculations using screened hydrogenic functions have been done by Burhop[2] with the difference that the effective charge of the active electron in his model is the same before and after ejection. Comparison with the experimental data as it will be discussed indicates that the choice made here for the effective charges for atoms with not-too-high atomic numbers is more justifiable.

The choice of the effective charge plays an important role in the behavior of the ionization cross section at high impact energies. This cross section behaves as $E^{-1}(A \ln E + B)$, with E the impact energy and A and B some atomic constants. The logarithmic term which is the dominating term is solely due to the atomic dipole potential which acts on the incident particle. The dipole moment of this potential in turn depends on the effective charge of the active electron before and after ejection. In Burhop's model the choice of the effective charge larger than unity for the final state leads to a smaller dipole potential and in turn to a smaller cross section compared to the cross sections calculated here. By an order of magnitude calculation it can be shown that for the majority of the high-energy collisions the time spent by the incident particle in the dipole field of the atom is comparable to the time for the active electron to cross the diameter of the atom.

During this crossing the atomic electron experiences different effective charges. Thus, while a final effective charge of unity for heavier elements and inner shell ionization may not be a good approximation, the choice of an effective charge equal to the initial effective charge is also questionable.

Other calculations using the Born approximation are due to McDowell,[3] Peach,[4] and McGuire.[5] In McDowell and Peach's calculational model the eigenfunction for the active electron before ejection is given by the Hartree-Fock calculations, and after ejection by a Coulomb function of charge unity. Thus in their model the active electron is in a non-Coulomb potential before ejection and in a Coulomb potential after ejection. In McGuire's calculation the active electron is in a Coulomb potential with variable charge before and after ejection.

The present calculation is similar to the McDowell and Peach calculations. In these calculations Hartree-Fock eigenfunctions are used for the initial state of the active electron while in our calculation we have used for this state the screened hydrogenic functions with effective charges given by the Hartree-Fock calculations. We expect that the two methods should produce similar results. This is substantiated by a number of comparisons that we have made between the results of the two methods. We also have accounted for the cross section for the production of doubly charged ions by considering that these ions are mainly produced by single inner-shell ionization with a subsequent ejection of an Auger electron. At high impact energies this appears to be a reasonable assumption.

II. FORMULATION

According to our model an atomic electron is specified by the hydrogenic quantum numbers nlm and an effective charge Z_e. Then starting from a general expression for the Born approximation given by Bethe[6] it can be shown, provided we neglect the interference terms between the ionization amplitudes of the atomic electrons, that the cross section per unit energy range of the ejected electron, $d\sigma/d\epsilon$, in an ionizing collision of a charged particle with charge $Z'e$, e being the magnitude of the electronic charge, with an atom with an active electron specified by nlm and Z_e, is given by

$$\frac{d[\sigma/(\pi a_0^2)]}{d(\epsilon/\mathcal{R}_\infty)}=\frac{4MZ'^2}{(2l+1)m_e a_0^5}\,\frac{(\epsilon/\mathcal{R}_\infty)^{1/2}}{E/\mathcal{R}_\infty}\int_{k_1-k_2}^{k_1+k_2}\frac{dq}{q^3}\times\int\sum_{m=0}^{l}(2-\delta_{m,0})\,|\langle f|1-e^{i\vec{q}\cdot\vec{r}}|nlm\rangle|^2\,d\hat{k}, \quad (1)$$

with σ the total cross section, ϵ the energy of the ejected electron, $\mathcal{R}_\infty=13.6$ eV, E and M the relative energy and reduced mass of the colliding system, and m_e the electronic mass. k_1 is the wave number of the relative motion before collision and is related to E by

$$k_1^2=a_0^{-2}(M/m_e)(E/\mathcal{R}_\infty)\ , \quad (2)$$

a_0 being the Bohr radius, and k_2 is the wave number of the relative motion after collision and is related to k_1 by

$$k_1^2-k_2^2=a_0^{-2}(M/m_e)(\Delta E/\mathcal{R}_\infty), \quad (3)$$

with ΔE the excitation energy. $\hbar\vec{q}=\hbar(\vec{k}_1-\vec{k}_2)$ is the momentum transfer between the particles, m is the absolute value of the magnetic quantum number of the atomic electron, and $\hat{k}$ is a unit vector in the direction of the ejected electron. $|nlm\rangle$ is the initial state of the active electrons and $|f\rangle$ is the final state given by

$$|f\rangle=|\vec{k}\rangle+\gamma\,|nlm\rangle\ , \quad (4)$$

where $|\vec{k}\rangle$ is a Coulomb wave function with charge unity normalized such that asymptotically it behaves as $(2\pi)^{-3/2}e^{i\vec{k}\cdot\vec{r}}$, with $\vec{r}$ the position vector of the atomic electron. Note should be taken that $|\vec{k}\rangle$ is a scalar. The constant γ is given by

$$\gamma=-\langle\vec{k}|nlm\rangle\ , \quad (5)$$

so that $\langle f|nlm\rangle=0$. Then while $|f\rangle$ has the same asymptotic form as $|\vec{k}\rangle$ it is orthogonal to $|nlm\rangle$. The state $|f\rangle$ would have been orthogonal to $|nlm\rangle$ if the two states had the same Hamiltonians. The forced orthogonalization will improve on the calculation. Also the first term in the bracket attributed to the interaction of the incident particle with the nucleus will drop out because of this orthogonalization. The momentum of the ejected electron is $\hbar k$ and is related to ϵ by the relation

$$|\vec{k}|^2=a_0^{-2}(\epsilon/\mathcal{R}_\infty)\ . \quad (6)$$

It is easy to see that σ has the dimension of the length squared.

From (4) and (5) we have that

$$\langle f|e^{i\vec{q}\cdot\vec{r}}|nlm\rangle=\langle\vec{k}|e^{i\vec{q}\cdot\vec{r}}|nlm\rangle-\langle\vec{k}|nlm\rangle\langle nlm|e^{i\vec{q}\cdot\vec{r}}|nlm\rangle\ . \quad (7)$$

It is easier to evaluate the first matrix on the right-hand side of (7) in parabolic coordinates and then transform it to the spherical coordinates. If the state vectors in the parabolic coordinates be specified by $|nn_1m\rangle$, with n_1 the usual quantum number in parabolic coordinates, then it follows immediately that

$$\langle\vec{k}|e^{i\vec{q}\cdot\vec{r}}|nlm\rangle=\sum_{n_1=0}^{n-m-1}\langle\vec{k}|e^{i\vec{q}\cdot\vec{r}}|nn_1m\rangle\langle nn_1m|nlm\rangle\ , \quad (8)$$

where the coefficients $\langle nn_1m|nlm\rangle$ are given through the Wigner's 3-j symbol by[7,8]

$$\langle nn_1m|nlm\rangle=(-)^m(2l+1)^{1/2}\begin{pmatrix}\frac{1}{2}(n-1) & \frac{1}{2}(n-1) & l\\ \frac{1}{2}(m-n_1+n_2) & \frac{1}{2}(m+n_1-n_2) & -m\end{pmatrix}\ , \quad (9)$$

with n_2 the other quantum number in parabolic coordinates related to n_1 by the relation $n_1+n_2=n-m-1$. The value of the matrix $\langle\vec{k}|e^{i\vec{q}\cdot\vec{r}}|nn_1m\rangle$ is given below:

$$\langle\vec{k}|e^{i\vec{q}\cdot\vec{r}}|nn_1m\rangle=\frac{-(2\alpha)^{m+2}e^{\pm im(\varphi_1+\varphi/2)}}{2(\pi Z_e)^{1/2}}\left[\frac{(n_2+m)\,!}{(n_1+m)\,!\,n_1\,!\,n_2\,!}\right]^{1/2}$$

$$\times\left(\frac{\beta}{1-e^{-2\pi\beta}}\right)^{1/2} q^m\,[1-(\hat{\mathrm{q}}\cdot\hat{\mathrm{k}})^2]^{m/2} A^{-m+i\beta}B^{-1-i\beta}\,\Sigma\;, \tag{10}$$

$$\Sigma=\sum_{\mu_1\geq\mu_2\geq\mu_3\geq\mu_4}^{n_1}\ \sum_{\nu_1}^{n_2}\ \sum_{\nu_2}^{m+\nu_1}(-)^{\mu_2+\nu_1}\quad(2\alpha)^{\mu_1+\nu_1}\quad C(\mu_4,\,\mu_3)$$

$$\times\binom{n_1}{\mu_1}\binom{n_2}{\nu_1}\binom{m+\nu_1}{\nu_2}\binom{\mu_1}{\mu_2}\binom{\mu_2}{\mu_3}\frac{(m+n_1)\,!\,(\nu_1+\nu_2)!\,\mu_4!}{(m+\mu_1)\,!\,(\nu_1+\nu_2-\mu_1+\mu_2)\,!}\ \frac{(m+\nu_1+\nu_2+\mu_2-\mu_3)\,!}{(m+\nu_1+\nu_2)\,!}$$

$$\times(2ik)^{\nu_1+\mu_4}\binom{i\beta+\nu_2}{\nu_2}\binom{-i\beta+m-1+\nu_1+\mu_4}{\mu_4}q^{2\mu_4}[1-(\hat{q}\cdot\hat{\mathrm{k}})^2]^{\mu_4}F\;, \tag{11}$$

$$F=A^{-\nu_1-\mu_4}B^{-\nu_2-\mu_2}D^{\mu_2-\mu_4}D^{*\nu_1+\nu_2-\mu_1+\mu_2}$$

$$\times\left[-\frac{2(\alpha+ik)(m+\nu_1+\mu_4-i\beta)}{A}-\frac{2\alpha(1+\mu_2+\nu_2+i\beta)}{B}+\frac{\mu_2-\mu_4}{D}+\frac{\nu_1+\nu_2-\mu_1+\mu_2}{D^*}\right]. \tag{12}$$

In these equations $\alpha=Z_e/na_0$, Z_e being the effective charge, $\beta=Z/ka_0$, where a_0 is the Bohr radius and $Z=1$ is the charge of the Coulomb field of the ejected electron, and A, B, and D are defined by

$$A=(\alpha+ik)^2+q^2,\;\; B=\alpha^2+(\vec{\mathrm{q}}-\vec{\mathrm{k}})^2,\;\; D=\alpha+i\hat{k}\cdot(\vec{\mathrm{q}}-\vec{\mathrm{k}})\;. \tag{13}$$

The constants $C(\mu_4,\,\mu_3)$ are given elsewhere.[9] ϕ_1 is the angle of azimuth of $\vec{\mathrm{q}}$ with respect to $\vec{\mathrm{k}}$ as the z axis. The lower limits of all the dummy variable integers in (11) are zero.

For evaluation of the second term on the right-hand side of (7) we notice that $\langle\vec{\mathrm{k}}\,|nlm\rangle$ can be obtained by making $|\vec{\mathrm{q}}\,|$ in the first term equal to zero. The second factor in this term can be evaluated by the usual methods. The matrices in (7) have been evaluated by taking the z axis along $\vec{\mathrm{k}}$. Then the second term on the right-hand side of (7) vanishes unless $m=0$.

In this way the matrix in (1) is evaluated and $d\sigma/d\epsilon$ is found accordingly. An integration of $d\sigma/d\epsilon$ with respect to ϵ will yield the total ionization cross section for ejection of an electron in a given atomic shell.

The effective charge for the atomic electron before ejection is found in the following way. Let Z_1 be the atomic number of the atom, then the effective charge Z_e is given by $Z_e=Z_1-S$, where S is the screening parameter representing screening of the nucleus by other atomic electrons. S is defined by Hartree[10] through the relation $R=R_H/(Z-S)$, with R some linear scale of the atomic wave function under consideration and R_H the corresponding value for the atomic hydrogen. It will be a good approximation to take R to be equal to the mean atomic radius $\bar{r}$. Froese[11] has assumed this to be the case, and gives S for several elements. We have used here values of S given by this author. For ionization of ions we have used the similar parameters given by Naqvi.[12] Effective charges and the ionization potentials of different atomic shells for the elements used here are given in Table I.

An examination of Eqs. (10)–(13) shows that the integrand on the right-hand side of (1) depends only on q, k, and the angle between $\vec{\mathrm{q}}$ and $\vec{\mathrm{k}}$. Then for evaluation of (1) a two-dimensional numerical integration, namely, integration with respect to this angle and q, is necessary. An additional integration with respect to ϵ will give the total cross section.

For ionization of ions we have used plane waves for the incident, and Coulomb waves for the ejected electrons. The use of the plane wave instead of the Coulomb wave for the incident particle is justifiable at high impact energies and the error incurred is of the same order as the error due to the use of the Born approximation. But the ejected electron wave function should be described by a Coulomb wave.

III. RESULTS AND DISCUSSION

The results of our calculations are presented in the following 18 figures. They are compared with the experimental data and with the results of some other representative quantum-mechanical calculations.

The experimental data up to 1966 have been collected and reviewed in an article by Kieffer and Dunn.[13] Much of the experimental data used here has been taken from this review and referred to this reference accordingly. A description of the results will now be given.

A. Differential Cross Sections

Before giving a description of the total cross sections it is instructive and a critical test of the theory to present results for the calculated differential cross sections and a comparision with the experimental data available.

In Fig. 1 the calculated differential cross sections for ionization of helium and neon by electron impact are given and compared with the recent measurements of Opal, Peterson, and Beaty.[14] These are relative measurements normalized by the experimenters.

TABLE I. Values of the effective charges Z_e and the ionization potentials (IP) employed.[a]

Atomic number	Element	Shell	Z_e	IP (eV)
2	He	$1s$	1.618	24.580
3	Li	$2s$	1.549	5.39
		$1s$	2.617	67.407
6	C	$2p$	2.869	11.264
		$2s$	3.784	19.375
7	N	$2p$	3.456	14.54
		$2s$	4.524	20.325
8	O	$2p$	4.035	13.614
		$2s$	5.260	28.44
10	Ne	$2p$	5.180	21.599
		$2s$	6.726	47.5
11	Na	$3s$	3.208	5.138
		$2p$	6.262	38.094
		$2s$	7.702	70.75
12	Mg	$3s$	4.150	7.644
		$2p$	7.299	58.2
		$2s$	8.691	96.2
18	Ar	$3p$	7.517	15.755
		$2s$	9.493	29.24
19	K	$4s$	4.577	4.339
		$3p$	8.700	24.63
		$3s$	10.571	40.8
30	Zn	$4s$	8.282	9.391
		$3d$	12.002	17.4
		$3p$	17.366	93.4
36	Kr	$4p$	11.785	13.996
		$4s$	14.730	27.6
		$3d$	19.06	96.86
37	Rb	$5s$	6.659	4.176
		$4p$	13.257	21.16
		$4s$	16.009	34.74
54	Xe	$5p$	15.612	12.127
		$5s$	18.930	23.4
55	Cs	$6s$	8.564	3.893
		$5p$	17.289	17.859
		$5s$	20.387	28.14
3	Li^+	$1s$	2.683	75.282

[a]The effective charges for atoms were taken from Ref. 11, and for Li^+ from Ref. 12. All outer-shell ionization potentials were taken from M. A. Lange, in *The Handbook of Chemistry*, 10th ed. (McGraw Hill, New York, 1961), p. 111. The inner-shell ionization were taken from the available photoionization data [cf. R. D. Hudson and L. J. Kieffer, JILA Information Report No. 11, University of Colorado, 1970 (unpublished)]. In other cases energy levels derived from x-ray data were used [cf. J. C. Slater, Phys. Rev. 98, 1039 (1955); J. A. Beardon and A. F. Burr, Rev. Mod. Phys. 39, 125 (1967)].

In the case of helium our calculation agrees fairly well with the experimental data except for the upturn seen at 50 eV in the experimental curve corresponding to the 100-eV primary energy. This upturn is most likely due to the exchange effect not taken into account in our calculation and which is important at the low impact energies.

In the case of neon the agreement is not as satisfactory as in the case of helium. In particular, the calculated curve seems to be flat in the region of low ejected electron energy. This is characteristic of the p-shell electron ionization in our model whose cross section dominates the neon, and also the carbon, nitrogen, and oxygen ionization differential cross sections. As is seen in the figure, the calculated cross section at low ejected electron energies is by as much as a factor of 2 higher than the measured values. The interesting feature of the figures is that the calculated and experimental curves cross each other. This leads to a better agreement between calculation and measurements for the total cross section as is evidenced in Fig. 5.

In Fig. 2 the calculated differential cross section for ionization of helium by proton impact is given and compared with the measurements of Rudd, Sautter, and Baily.[15] As can be seen except at very low ejected electron energies the agreement is quite satisfactory. A more elaborate calculation on differential cross sections for the ionization of helium by electron and proton impact with an accurate wave function has been done by Bell, Freeston, and Kingston.[16] The amount of agreement of the results of Bell *et al.* with the data of Rudd *et al.* is comparable to the agreement that we have found in our comparison with these data. A classical three-body calculation has been carried out by Bonsen and Banks[17] with excellent agreement with the measurements for small and intermediate ejection angles and all ejection energies.

When both the incident and ejected electron energies are large compared to the ionization potential, the differential cross section is given by the Rutherford formula given by the mass-independent expression[18]

$$\frac{d\sigma/(\pi a_0^2)}{d(\epsilon/\mathfrak{R}_\infty)} = 4Z'^2\left(\frac{v_0}{v}\right)^2\left(\frac{\mathfrak{R}_\infty}{\epsilon}\right)^2, \quad \epsilon \leqslant 2M^2v^2/m_e \tag{14}$$

with Z' and M defined before, v the incident velocity, and $v_0 = \hbar/(m_e a_0)$. For large ϵ our calculated values given in Fig. 2 agree with the above formula within a few percent.

In Fig. 3 we have made a comparison between the measured and calculated photoionization cross

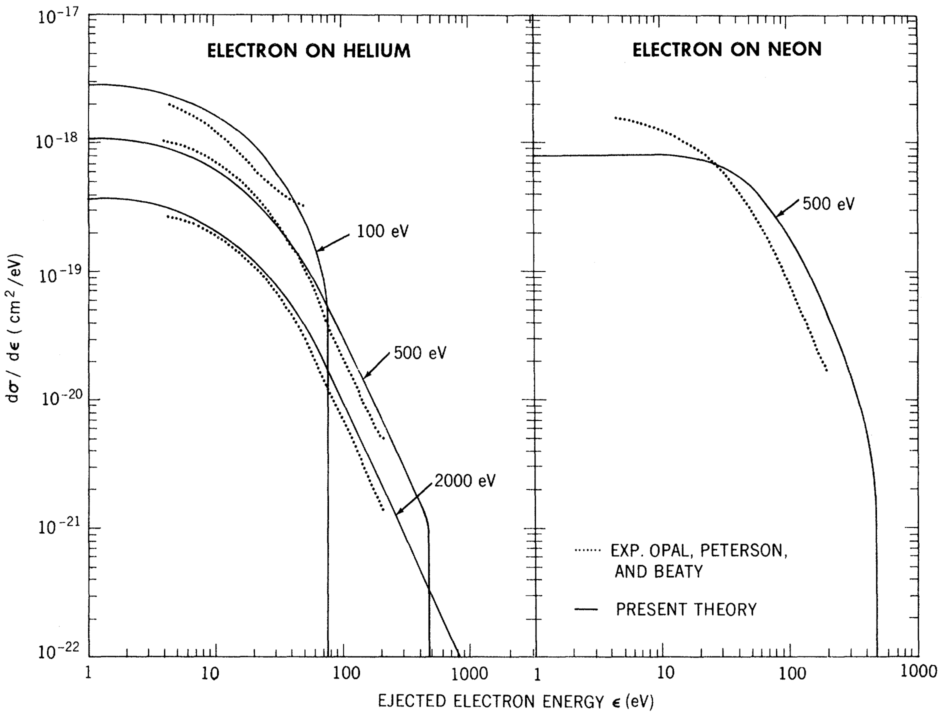

FIG. 1. Cross section per unit energy range of the ejected electrons in ionization of helium and neon by electron impact. The energy of the primary, in eV, is marked on each curve. The measurements are due to Opal, Peterson, and Beaty (Ref. 14).

section for lithium. The calculation has been made using our model for the atom. We do not intend here to do a photoionization calculation, since our model is too crude for such calculations. But since $d\sigma/d\epsilon$ at high impact energies is related for not too large values of ϵ to the photoionization

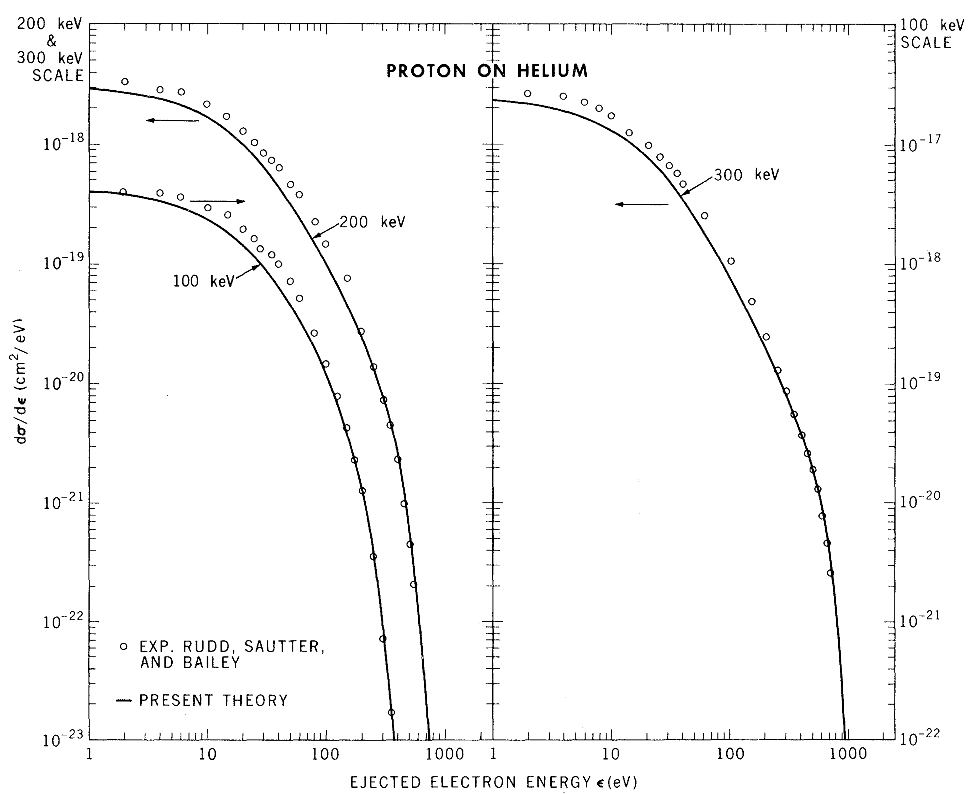

FIG. 2. Cross sections per unit energy range of the ejected electrons in ionization of helium by proton impact. The experimental data are due to the absolute measurement of Rudd, Sautter, and Bailey (Ref. 15).

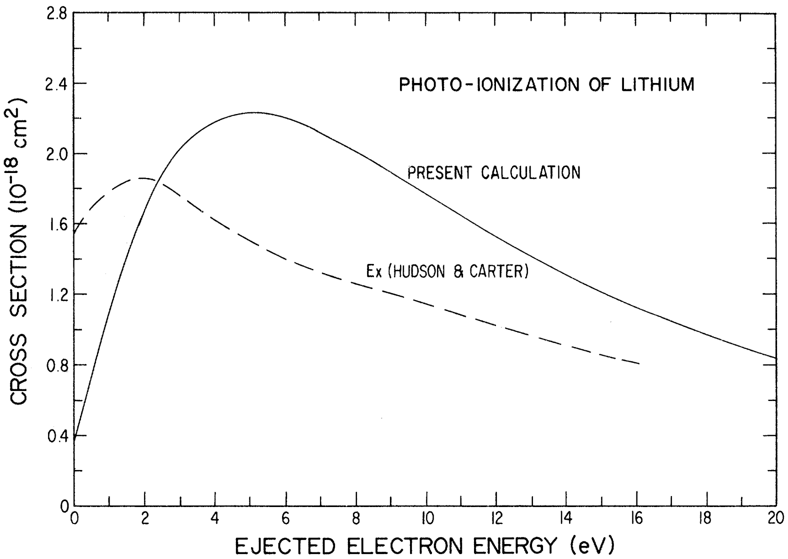

FIG. 3. Photoionization of lithium. Measurement of Hudson and Carter (Ref. 19) is compared with our calculation.

cross section, the comparison is an indication of the agreement that we should expect for the differential cross section. Owing to the crossing of the two curves, we should expect better agreement for the total cross section than the differential cross section. Further, the calculated value for the total cross section should be higher than measurements. This is in contrast to what is seen in Fig. 9. This point will be discussed in more details later on.

B. Inert Gases

Our results for the inert gases are given in Fig. 4–6. Source for all the experimental data, except those of Goudin and Hagemann[20] and Schram,[21] is Ref. 13.

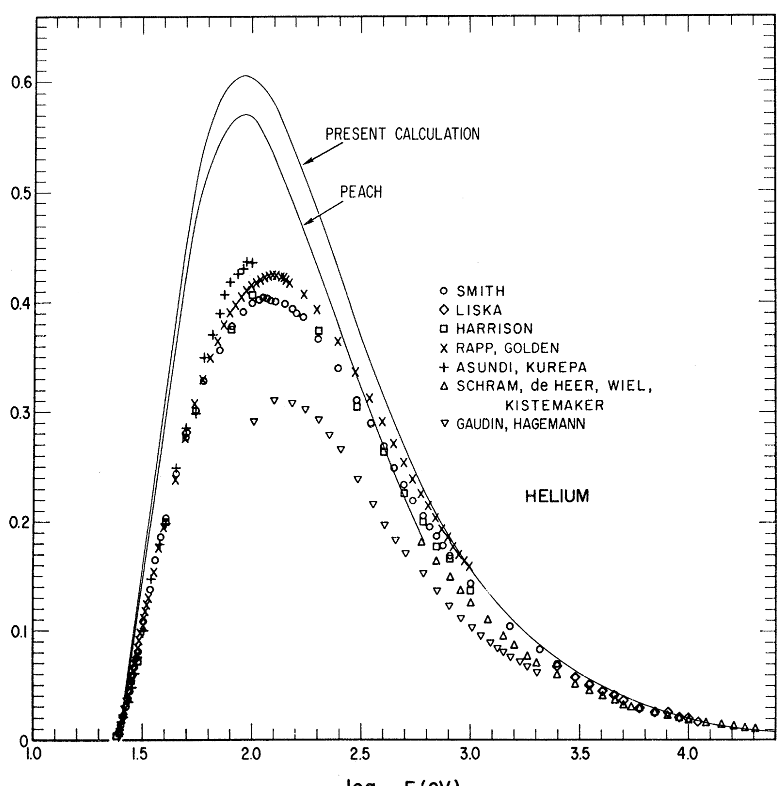

FIG. 4. Ionization of helium by electron impact. In this and all the following figures σ is the ionization cross section in units of πa_0^2, and E is the impact energy in units of eV. All the experimental data in this figure and the following two figures are absolute measurements. For a description see Ref. 13, except the data of Goudin and Hagemann which is described in Ref. 20. The two solid lines are calculations of Peach (Ref. 22) and ours.

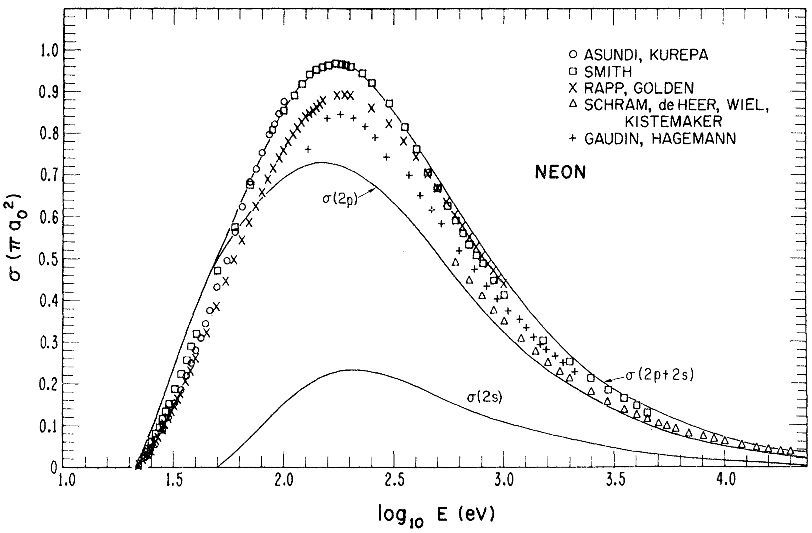

FIG. 5. Ionization of neon by electron impact. See Refs. 13 and 20 for a description of the measurements. In this and all the following figures $\sigma(nl)$ refers to the present calculation and is the cross section due to the nl shell ionization. $\sigma(nl+n'l')$ is the sum of $\sigma(nl)$ and $\sigma(n'l')$, etc.

The experimental data displayed for He, Ne, and Ar represent total experimental cross sections and are, respectively, about 2%, 10%, and 12–15% higher than the observed single ionization cross sections in the energy range from 500 to several thousand eV.

In these figures we have presented the results of our calculation and calculations of Peach for helium,[22] and for sodium and potassium.[4]

In Fig. 7 we have plotted $E\sigma$ vs $\log_{10}E$ for electron-impact ionization of He, Ne, and Ar. σ is the experimental or the theoretical single ionization cross section. The figure shows that for helium the three calculations give almost the same results. For neon the new (unpublished) calculated cross section of Peach is slightly higher than ours. For both neon and argon the results of McGuire's calculation agree better with the experimental results.

In Fig. 8 we compare our results for the single $3d$-shell ionization in krypton with the data of Tate and Smith,[24] Schram,[21] and El-Sherbini *et al.*[25] for production of doubly charged ions in krypton. One solid line corresponds to a final effective charge of unity; the other corresponds to a final charge equal to the initial effective charge.

Since at high impact energies most collisions take place with small momentum transfer, for these energies substantial amounts of the produced doubly charged ions are due to the single inner-

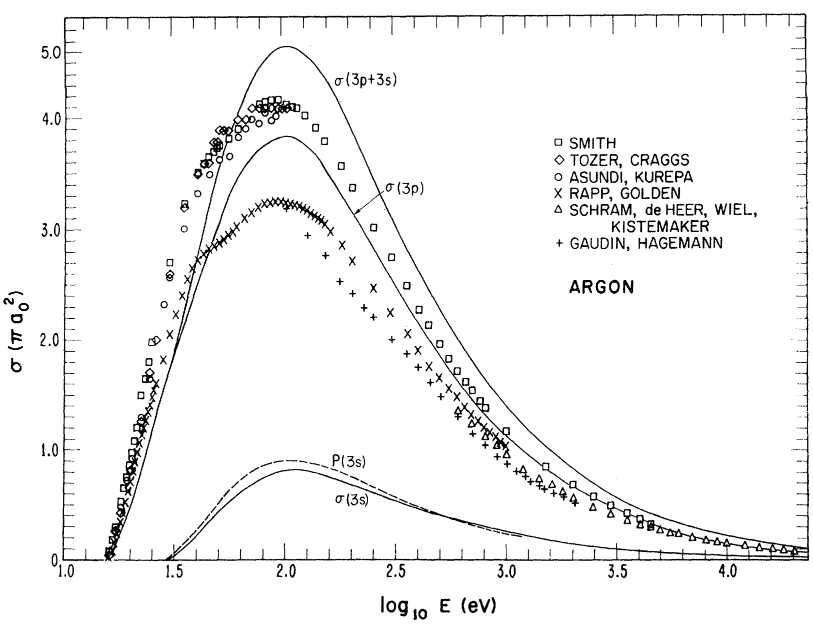

FIG. 6. Ionization of argon by electron impact. See Refs. 13 and 20 for a description of the measurements. $P(3s)$ is calculation of Peach (Ref. 4) and it gives $\sigma(3s)$. In $P(3s)$ autoionization has also been taken into account.

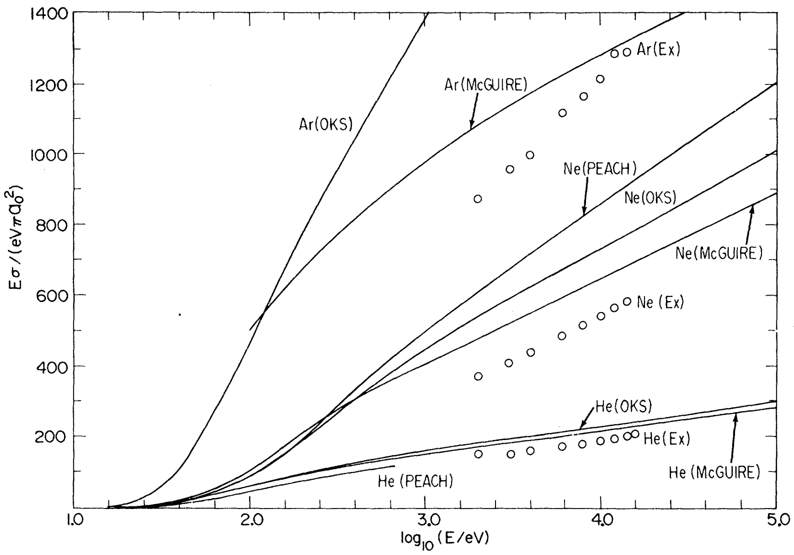

FIG. 7. Bethe plot for the ionization of helium, neon, and argon by fast (nonrelativistic) electrons. The experimental data shown by circles are for the production of singly charged ions and are due to Van der Wiel, El-Sherbini, and Vriens (Ref. 23). Solid lines are the results of our calculations, marked OKS, and calculations of McGuire (Ref. 5) and Peach (Ref. 22 for He, and new unpublished results for Ne).

shell ionization followed by an Auger process. This is the justification for our comparison. While the agreement found between the curve $Z=1$ and the data of El-Sherbini *et al.* may very well be accidental, it seems that the curve $Z=Z_e$ gives too small a cross section. It was pointed out in the introduction that the choice $Z=Z_e$ corresponds to a too small atomic dipole potential which in turn leads to a too small cross section.

C. Alkalides

In Figs. 9–11 ionization cross sections of Li, Na, and K are given. In Fig. 9 our results for both shell ionizations agree better with the absolute measurement of McFarland and Kinny[26] than the results of McDowell *et al.*[30] marked by MMP (2*s*). However, it was pointed out in the discussion of Fig. 3 that based on the photoionization data we should expect our calculated curves to lie above the experimental curve. Figure 9 shows the opposite situation. This suggests inconsistencies between photoionization and electron-impact ionization data. In their recent measurement on electron-impact ionization of lithium, Jalin, Hagemann, Lohez, and Botter[33] find disagreement with the data of McFarland *et al.* Their measurement indicates smaller cross sections at high impact energies, and is in agreement with the data of McDowell *et al.*

In Fig. 10 cross sections for production of singly and doubly charged sodium ions are presented. Similar to the discussion of Fig. 8 we have assumed

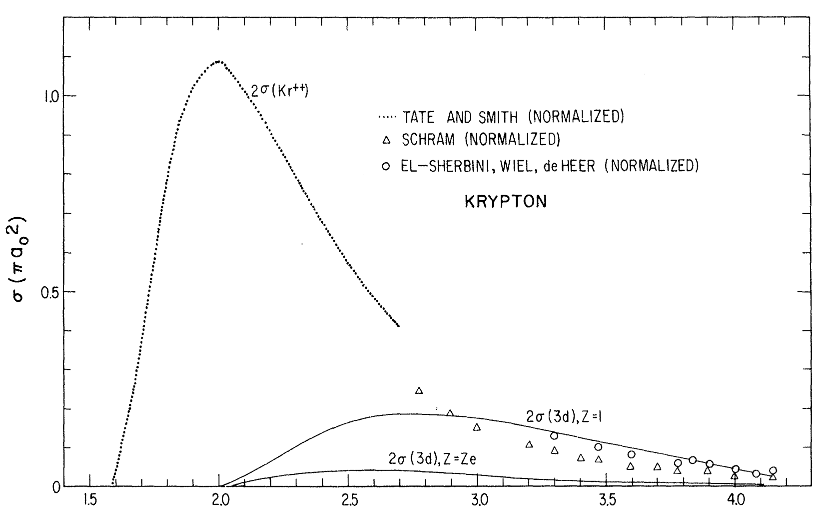

FIG. 8. Production of the doubly charged krypton ions by electron impact. $2\sigma(Kr^{++})$ and triangles and circles give twice the relative measured cross section for production of the doubly charged ions. The measurements are due to Tate and Smith (Ref. 24), Schram (Ref. 21), and El-Sherbini *et al.* (Ref. 25). The two solid curves correspond to the present calculation, one for $Z=1$, and the other for $Z=Z_e$, and they give $2\sigma(3d)$. Z is the final-state charge of the atomic electron.

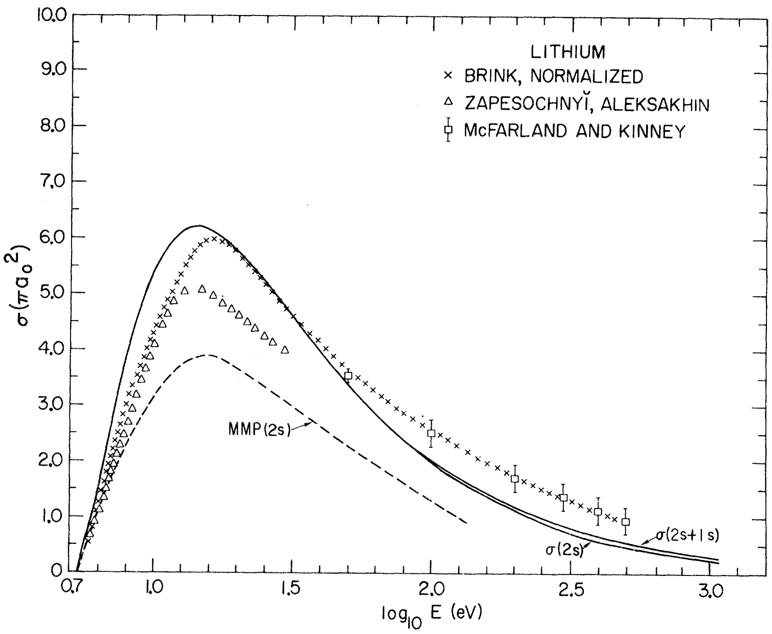

FIG. 9. Ionization of lithium by electron impact. Measurements of McFarland and Kinney (Refs. 13, 26, and 27) and Zapesochnyi and Aleksakhin (Ref. 28) are absolute total experimental cross sections; those of Brink (Ref. 29) are relative normalized to the results of McFarland *et al.* MMP($2s$) is the outer shell ionization calculation of McDowell *et al.* (Ref. 30).

that a single $2s$ shell ionization will lead to the production of doubly charged ions. Hence $2\sigma(2s)$ is compared to $\sigma(Na^{++})$, and partial agreement is obtained. Based on this assumption the cross section for production of total ionic current comprising Na^+ and Na^{++} is given by $\sigma(3s+2p)+2\sigma(2s)$. This cross section has been compared to the data of McFarland *et al.*

In Fig. 11 ionization of K is presented. Explanation is the same as in Fig. 10.

In Fig. 12 a Bethe plot, similar to Fig. 7, is constructed for Li, Na, and K. For Li the experimental cross sections in their range are larger than the four sets of the calculated results. It is

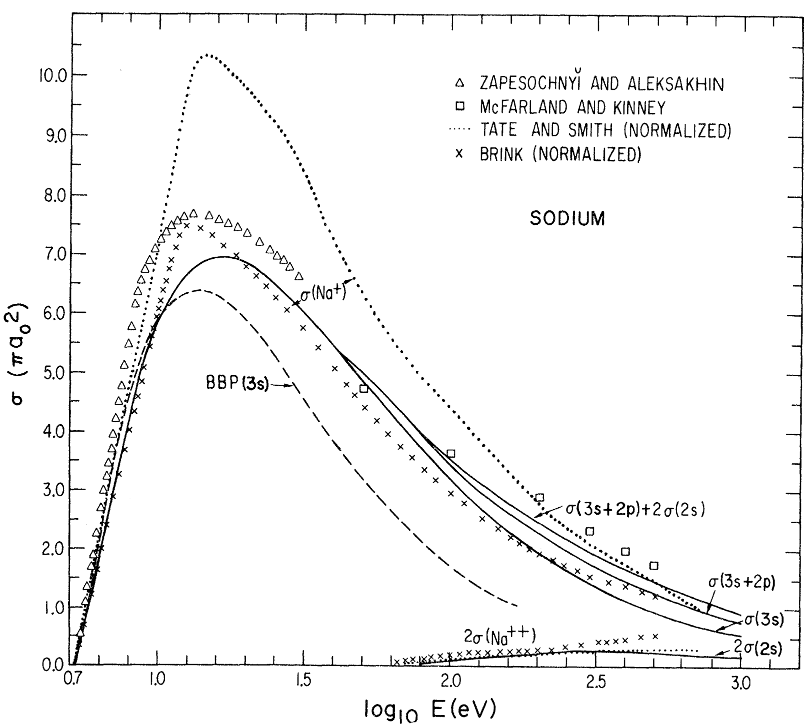

FIG. 10. Ionization of sodium by electron impact. Measurements of McFarland and Kinney (Refs. 13, 26, and 27) and Zapesochnyi and Aleksakhin (Ref. 28) are absolute total experimental cross sections. Those of Tate and Smith (Ref. 24) and Brink (Ref. 29) are the cross sections for the production of the ions Na^+ and Na^{2+}. They are relative and are normalized at 500 eV to the results of McFraland and Kinney. $\sigma(3s+2p)$ is to be compared to the experimental $\sigma(Na^+)$ curves. $\sigma(3s+2p)+2\sigma(2s)$ gives the sum of $\sigma(3s)$, $\sigma(2p)$, and $2\sigma(2s)$, and should be compared with the measured total ionization cross section. For an explanation see the text. BBP($3s$) is calculation of Bates *et al.* (Ref. 31) for $\sigma(3s)$.

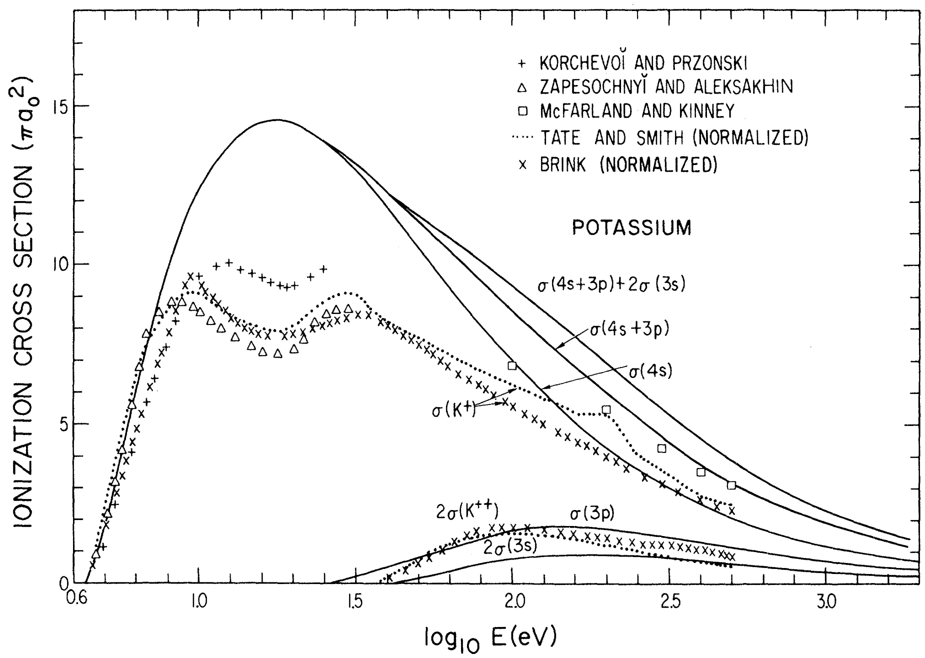

FIG. 11. Ionization of potassium by electron impact. The measurement of Korchevoi and Prozonski (Ref. 32) is absolute. For other measurements see Fig. 10. Explanation is similar to Fig. 10.

likely that the experimental values are too large (cf. Ref. 31). For K the experimental data shown in Fig. 12 are lower than the calculated results. This may be due to the unreliability of our model for K ionization.

D. Magnesium and Zinc

In Figs. 13 and 14 our results for ionization of magnesium and zinc are shown. As is seen in Fig. 13 our calculated curve marked $\sigma(3s)$ for single ionization of magnesium is in fair agreement with the measurement at high impact energies, but near the peak calculated results are substantially lower than the measurement. Comparison of Figs. 13 and 10 is instructive. Sodium has one and magnesium has two outer-shell s electrons. In the case of the ionization of sodium shown in Fig. 10 the calculated and measured curves at the peak are in good agreement in their shapes as well as in their magnitudes, contrary to the situation in magnesium. The difference can be attributed to the possible double excitation in the magnesium

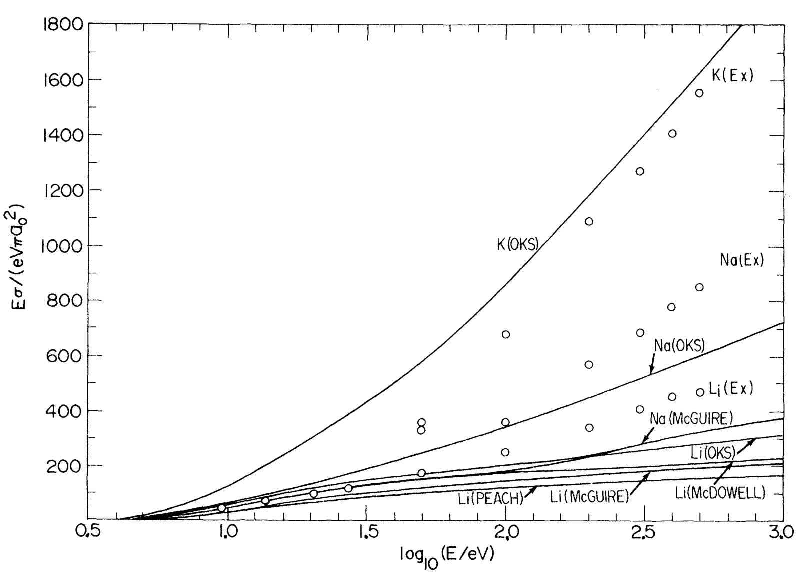

FIG. 12. Bethe plot for ionization of lithium, sodium, and potassium by fast (nonrelativistic) electrons. The experimental data shown by circles are due to McFarland and Kinney (Ref. 13). Solid lines are the results of our calculation, marked OKS, McGuire (Ref. 5), McDowell (Ref. 3), and Peach (Ref. 22). Note should be taken that the experimental data are for total ionic current while calculations are for single ionization.

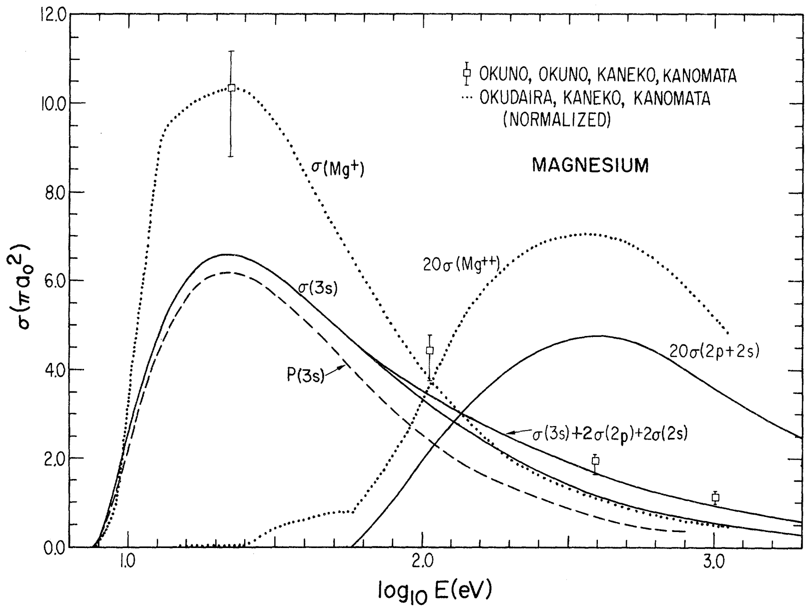

FIG. 13. Ionization of magnesium by electron impact, $\sigma(\mathrm{Mg}^{+})$ and $20\sigma(\mathrm{Mg}^{++})$ curves give cross sections for production of singly and doubly charged ions, the cross section for the latter curve being multiplied by a factor of 20. The measurement of Okuno *et al.* (Ref. 34) is the absolute total ionization cross section. The relative measurements of Okudaira *et al.* (Ref. 35) were normalized by the experimenters at 500 eV to the results of Okuno *et al.* $P(3s)$ is calculation of Peach (Ref. 4), and it gives $\sigma(3s)$.

outer shell, with a subsequent autoionization. Measurements of Kaneko[36] (not shown in the figure) indicate the presence of a number of autoionization lines from threshold up to the peak of the ionization curve.

In Fig. 13 it is also seen that the cross section for production of doubly charged ions compared to singly charged ions in magnesium is much larger than the same quantity for sodium. While for sodium the doubly charged current accounts for only 20% of the total cross section at high energies, in magnesium it is 50%. The difference is most likely due to the fact that in Mg the ejection of a $2p$ electron can be followed by the emission of a $3s$ electron through an Auger process. This cannot take place in sodium since the energy gap between $2p$ and $3s$ in sodium is not wide enough to make the process operational, and also owing to the fact that there is only one $3s$ electron in sodium.

Vacancies in the $2p$ and $2s$ shells is thought to lead to the formation of the doubly charged ions through the Auger process. The fact that the $\sigma(\mathrm{Mg}^{++})$ curve lies above the $\sigma(2p+2s)$ curve, although commonly our calculated cross sections overestimate the actual cross sections, is an in-

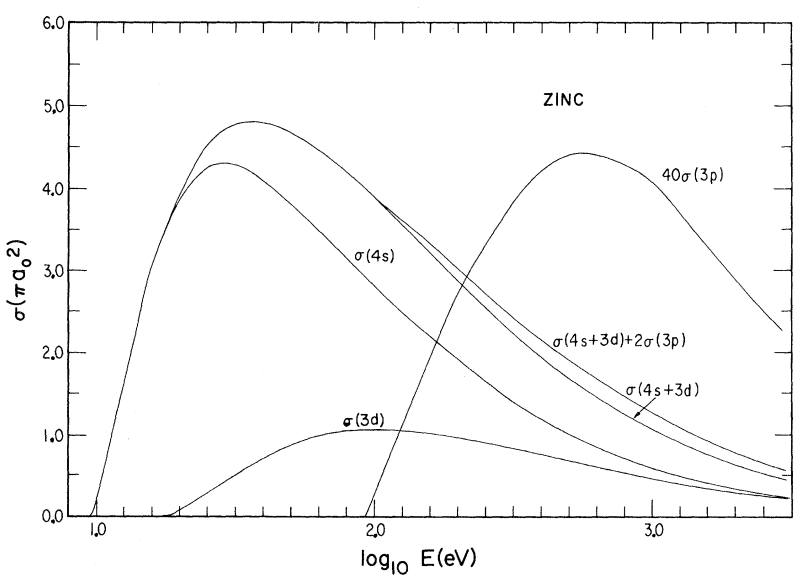

FIG. 14. Ionization of zinc by electron impact. Symbols the same as in Fig. 5.

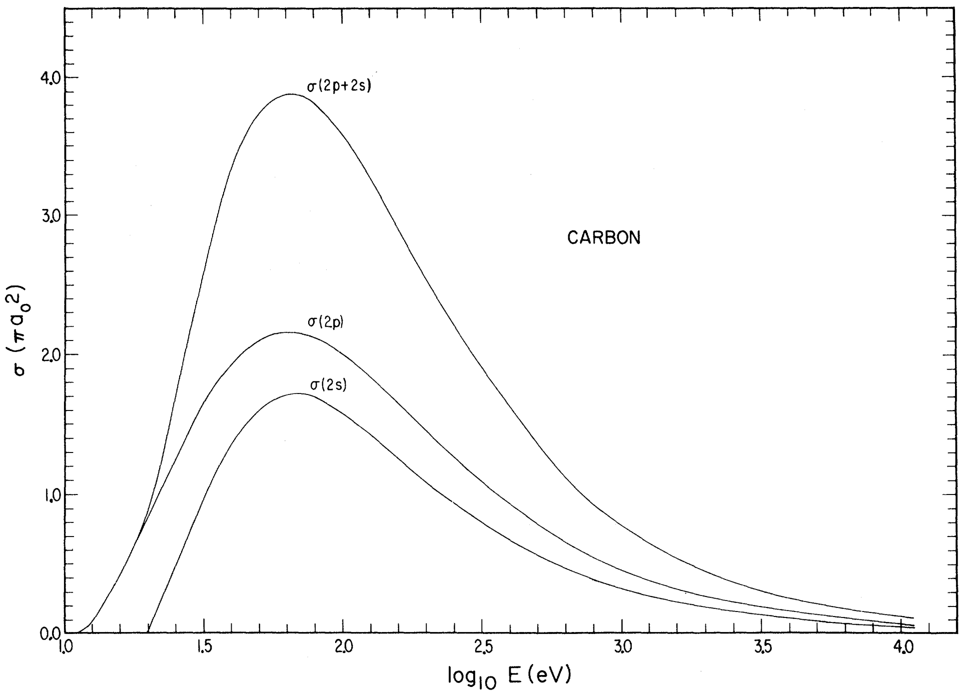

FIG. 15. Ionization of carbon by electron impact. Symbols the same as in Fig. 5. No measurement is available on ionization of this element.

dication that other mechanisms besides single ionization are important for the production of doubly charged ions in the energy range given here.

Figure 14 gives calculated cross sections for the ejection of $4s$, $3d$, and $3p$ electrons in zinc. No absolute measurement on the ionization of zinc is available. Photoionization data on Zinc[37] indicate that the element is rich in autoionization states at the low energy side of the peak of the ionization cross section. We then anticipate that the peak in the measured ionic current will be higher than the peak of the curve marked $\sigma(4s+3d) + 2\sigma(3p)$. As usual we have assumed that $3p$-shell electron ionization will lead to the production of doubly charged ions through the Auger process. For this reason $\sigma(3p)$ has been multiplied by a factor of 2 before being added to the cross section for the total ionic current.

E. Carbon, Nitrogen, and Oxygen

Figures 15–17 give our results for single ionization of carbon, nitrogen, and oxygen. No experimental data are available for carbon. It is important to note that in these three elements contribution to the ionization cross section of the $2s$ shell is almost as important as the $2p$ shell, and in any calculation the two shells should be taken into account.

In Figs. 16 and 17 Bethe plots for the calculated and the experimental data for nitrogen and oxygen are shown. Differential cross section $d\sigma/d\epsilon$ for C, N, and O which find usefulness in atmospheric physics and astrophysics are available,[38] but because of the space limitation they will not be given here.

F. Ionization of Ions

In the ionization of ions the incident particle should be described by a Coulomb wave function . At high impact energies the Coulomb wave can be replaced by a plane wave. It can be shown that

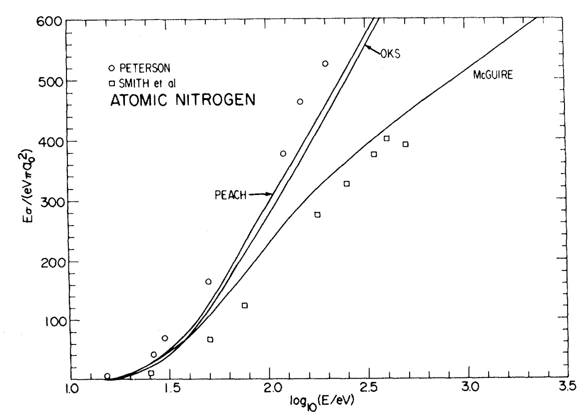

FIG. 16. Bethe plot for ionization of atomic nitrogen by electron impact. Measurement of Smith *et al.* is for the total ionic current while that of Peterson is for N^+ current. For a description of the experimental results see Ref. 13. Solid lines are the results of our calculations of McGuire (Ref. 5) and Peach (unpublished).

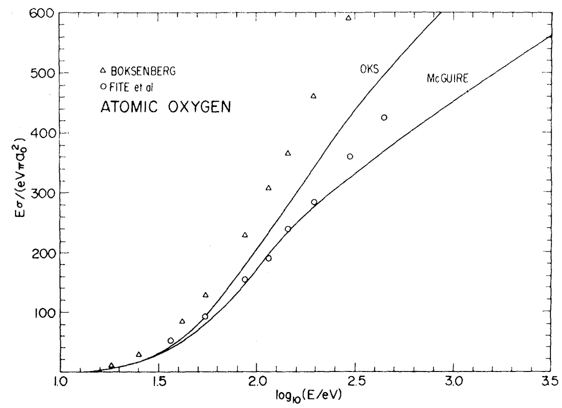

FIG. 17. Description is similar to Fig. 16. The experimental data are taken from Ref. 13 and are for single ionization.

the resultant inaccuracy is comparable to the inaccuracy in the Born approximation. This has been verified by Peart, Walton, and Dolder[39] who have compared their absolute cross-section measurement of electron impact ionization of He^+ with a Born calculation where a plane wave is used for the incident electron.

Here we apply our model to the ionization of a nonhydrogenlike ion, namely, Li^+. The effective charge and ionization potential of Li^+ necessary in our calculation is given in Table I.

In Fig. 18 we have constructed a Bethe plot for ionization of Li^+ by electron impact. Measured cross sections are by Peart *et al.* (Ref. 39) and by Peart and Dolder.[40] The measurement is well extended into the relativistic region. When the projectile has relativistic energies, the target, excluding the inner shell of heavy atoms and ions, can still be treated nonrelativistically. The relativistic correction for the projectile has been made by Bethe.[41] The nonrelativistic high-energy inelastic atomic cross section according to Bethe[6] is given by $\sigma = E^{-1}(A \ln E + B)$, with E the relative kinetic energy of the system, and A and B some atomic constants. For relativistic projectiles this expression should be replaced by

$$(\tfrac{1}{2}mv^2)\,\sigma = A\{\ln[\tfrac{1}{2}mv^2/(1-\beta^2)] - \beta^2\} + B, \qquad (15)$$

with m and v the rest mass and velocity of the projectile, $\beta = v/c$, c being the speed of light, and A and B the nonrelativistic atomic constants.

In Fig. 18 the straight line R is a plot of the left-hand side versus the expression in the curly bracket in (15). The slope and the intersection of R gives A and B. It has been obtained by constructing a segment of R in the nonrelativistic high-energy region, using for σ the computed Born cross section. By extension of the segment R has been obtained. The curve NR has been obtained by using for σ the computed Born cross section throughout the range of the curve. The departure of the NR from the R curve at high impact energy is a measure of the amount of the relativistic correction.

If the relativistic correction were not necessary the experimental points should fall on the NR curve, assuming the accuracy of our nonrelativistic calculation. With relativistic correction the experimental data should agree with R. Although

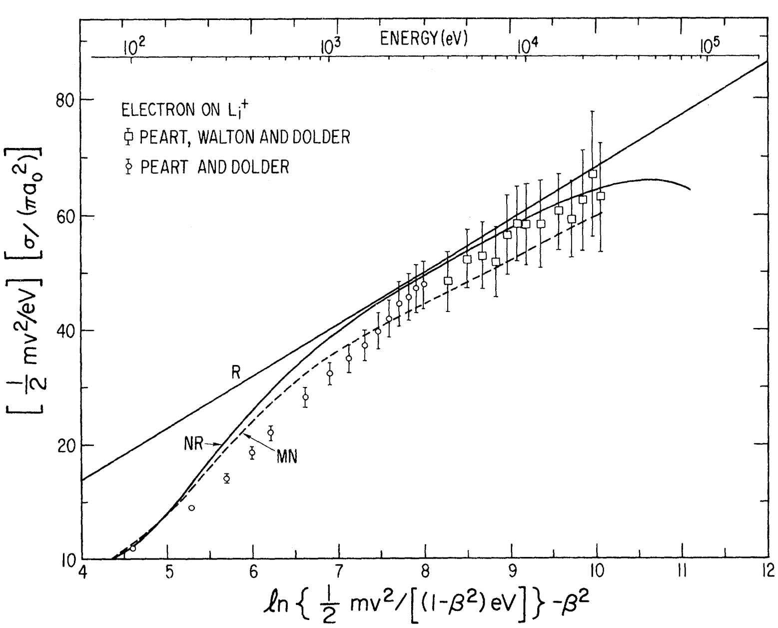

FIG. 18. Ionization of lithium ion by electron impact. The experimental cross section for production of Li^{++} is due to the absolute measurements of Peart, Walton, and Dolder (Ref. 39), and Peart, and Dolder (Ref. 40). R represents our calculation with relativistic correction. NR is our nonrelativistic Born calculation. Presented also are calculations of Moores and Nussbaumer (Ref. 42) shown by MN curve in the figure. For other calculations see Ref. 39.

the experimental data are extended to the relativistic region because of their error bars the correctness of the relativisitic correction cannot be verified, and this verification is left to the future.

IV. CONCLUSION

By using a simple model it has been shown that reasonable values for the total high-energy ionization cross sections for atoms with not-too-high atomic numbers can be obtained. We find close agreement with the results of McDowell and Peach whose model is similar to ours except that they use Hartree-Fock wave functions for the initial state of the atomic electron. The ionization amplitude in the present model is in analytic form and is amenable to further analysis. For atoms with intermediate atomic numbers, the calculation of McGuire seems to give better agreement with the experimental data compared to other calculations.

We have also applied our model to the electron-impact ionization of Li^+, and satisfactory agreement with the experimental data is obtained.

[1]K. Omidvar and E. C. Sullivan, in *Abstract of Papers of the Fifth International Conference on the Physics of Electronic and Atomic Collisions* (Publishing House Nauka, Lenningrad, USSR, 1967). In this reference an error in the algebra has led to errors in the ionization cross sections of Li and Hg. This error was discovered by one of us (H. L. K.). It has been corrected in the present article. Also, K. Omidvar and H. L. Kyle, *Abstract of Papers of the Seventh International Conference on the Physics of Electronic and Atomic Collisions* (North-Holland, Amsterdam, 1971).

[2]E. H. S. Burhop, Proc. Cambridge, Phil. Soc. 36, 43 (1940).

[3]M. R. C. McDowell, in *Case Studies in Atomic Collision Physics* 1, edited by E. W. McDaniel and M. R. C. McDowell (North-Holland, Amsterdam, 1969).

[4]G. Peach, J. Phys. B 1, 1088 (1968); 3, 328 (1970). We have been informed by the author that the *p* ionization results in these references are in error. For this reason these results will not be reproduced here. For the new (unpublished) results see Figs. 7 and 16.

[5]E. J. McGuire, Phys. Rev. 3, 267 (1971).

[6]H. A. Bethe, Ann. Physik 5, 325 (1930).

[7]A. O. Barut and H. Kleinert, Phys. Rev. 160, 1149 (1967).

[8]J. W. B. Hughes, Proc. Phys. Soc. (London) 91, 810 (1967).

[9]K. Omidvar, Phys. Rev. 140, A26 (1965), Table I.

[10]D. R. Hartree, Proc. Cambridge Phil. Soc. 51, 684 (1955).

[11]C. Froese, J. Chem. Phys. 45, 1417 (1966); also, University of British Columbia, Department of Mathematics, Technical Note (unpublished).

[12]A. M. Naqvi, J. Quant. Spectry. Radiative Transfer 4, 597 (1964); also, A. M. Naqvi and G. A. Victor, Air Force Weapons Laboratory, Kirkland Air Force Base, New Mexico, Technical Document Report No. TDR-63-3118 (unpublished).

[13]L. J. Kieffer and G. H. Dunn, Rev. Mod. Phys. 38, 1 (1966).

[14]C. B. Opal, W. K. Peterson, and E. C. Beaty, University of Colorado JILA Report No. 108, 1971 (unpublished).

[15]M. E. Rudd, C. A. Sautter, and C. L. Bailey, Phys. Rev. 151, 20 (1966).

[16]K. L. Bell, M. W. Freeston, and A. E. Kingston, J. Phys. B 3, 959 (1970).

[17]T. F. M. Bonsen and D. Banks, J. Phys. B 4, 706 (1971).

[18]E. Gerjuoy, Phys. Rev. 148, 54 (1966).

[19]R. D. Hudson and V. L. Carter, J. Opt. Soc. Am. 57, 651 (1967).

[20]A. Goudin and R. Hagemann, J. Chim. Phys. 64, 1209 (1967).

[21]B. L. Schram, Physica 32, 197 (1966).

[22]G. Peach, Proc. Phys. Soc. (London) 87, 381 (1966).

[23]M. J. Van der Wiel, T. M. El-Sherbini, and L. Vriens, Physica 42, 411 (1969).

[24]J. T. Tate and P. T. Smith, Phys. Rev. 46, 773 (1934).

[25]T. M. El-Sherbini, M. J. Van der Wiel, and F. J. DeHeer, Physica 48, 157 (1970).

[26]R. H. McFarland and J. D. Kinney, Phys. Rev. 137, A1058 (1965). Cross sections for single ionization of sodium, rubidium, and cesium given in this reference are in error. For corrected values see Ref. 27.

[27]R. H. McFarland, Phys. Rev. 139, A40 (1965).

[28]I. P. Zapesochnyi and I. S. Aleksakhin, Zh. Eksperim. i Teor. Fiz. 55, 76 (1968) [Sov. Phys. JETP 28, 41 (1969)].

[29]G. O. Brink, Phys. Rev. 127, 1204 (1962).

[30]M. R. C. McDowell, V. P. Myerscough, and G. Peach, Proc. Phys. Soc. (London) 85, 703 (1965).

[31]D. R. Bates, A. H. Boyd, and S. S. Prasad, Proc. Phys. Soc. (London) 85, 1121 (1965).

[32]Y. P. Korchevoi and A. M. Prozonski, Zh. Eksperim. i Teor. Fiz. 51, 1617 (1966) [Sov. Phys. JETP 24, 1089 (1967)].

[33]R. Jalin, R. Hagemann, P. Lohez, and R. Botter, in *Abstracts of Papers of the Seventh International Conference on the Physics of Electronic and Atomic Collisions* (North-Holland, Amsterdam, 1971).

[34]Y. Okuno, K. Okuno, Y. Kaneko, and I. Kanomata, J. Phys. Soc. Japan 29, 164 (1970).

[35]S. Okudaira, Y. Kaneko, and I. Kanomata, J. Phys. Soc. Japan 28, 1536 (1970).

[36]Y. Kaneko, J. Phys. Soc. Japan 16, 2288 (1961).

[37]G. V. Marr and J. M. Austin, J. Phys. B 2, 107 (1968).

[38]K. Omidvar, H. L. Kyle, and E. C. Sullivan, Goddard Space Flight Center Report No. X-641-71-145 (unpublished).

[39]B. Peart, D. S. Walton, and K. T. Dolder, J. Phys. B 2, 1347 (1969).

[40]B. Peart and K. T. Dolder, J. Phys. B 1, 872 (1968).

[41]N. F. Mott and H. S. W. Massey, *The Theory of Atomic Collisions*, 3rd ed. (Clarendon Press, Oxford, England, 1963), p. 815.

[42]D. L. Moores and H. Nussbaumer, J. Phys. B 3, 161 (1970).